Raman scattering and hydrogen-content analysis of amorphous hydrogenated carbon films irradiated with 200-keV C^+ ions

Leonilda A. Farrow, Barry J. Wilkens, Antoni S. Gozdz, and Derrick L. Hart
Bellcore, Red Bank, New Jersey 07701-7040
(Received 16 June 1989; revised manuscript received 10 January 1990)

Amorphous hydrogenated "diamondlike" carbon films (*a*-C:H) have been modified by bombardment with 200-keV C^+ ions at four doses ranging from 10^{14} to 10^{17} cm^{-2}. Ratios of carbon to hydrogen in the resulting samples have been determined with use of elastic recoil detection (ERD) and Rutherford backscattering (RBS); hydrogen content is significantly reduced as the dose is increased. Raman scattering data indicate increasing graphitization with increasing ion dose. These data have been analyzed to determine position and width of previously observed *G* and *D* lines. Raman scattering results obtained for *a*-C:H films annealed at temperatures up to 800 °C indicate that C^+-ion bombardment and high-temperature annealing of *a*-C:H films have a similar effect on their structure. Data obtained from all of the measurement techniques cited above indicate that the major changes occur in the *a*-C:H films implanted with doses of 10^{16} cm^{-2} or greater.

I. INTRODUCTION

The amount of interest and research in the field of hard carbon films, loosely termed "diamondlike" or amorphous hydrogenated carbon films[1,2] (*a*-C:H), continues to be high as new processes for deposition and analysis lead to more extensive applications.[3] The fundamental difference between these films and true diamond is the presence of varying amounts of trigonal, or graphitic, bonds as well as a rather high (5–50 at. %) hydrogen content. These features lead to a wide range of physical characteristics in the films. In order to obtain films with mechanical, electrical, and optical properties approaching those of diamond, film-deposition conditions should be optimized to provide films with a minimum hydrogen content and a maximum fraction of tetragonal bonding.[3,4] Changes in the proportion of trigonal to tetragonal bonding as well as crystallite growth in the originally amorphous films have been previously reported as a function of annealing at various temperatures.[5] All of these changes have been monitored by Raman scattering,[5] where the position and relative strengths of specific vibrational modes are directly related to the formation of small graphite crystals and to bond-angle disorder.[5,6] Recently the effect on *a*-C:H films of bombardment with fluorine,[7] gold,[7] hydrogen,[8] and nitrogen[8] ions has been studied using Rutherford backscattering (RBS),[7] proton recoil detection,[7] infrared transmittance,[8] and photoluminescence.[8] In this report we describe modification of *a*-C:H films by ion implantation as well as by rapid thermal annealing (RTA), and present detailed Raman scattering results to describe the graphitization process as a function of ion dose and annealing temperature.

II. EXPERIMENT

Amorphous hydrogenated carbon films were deposited onto a variety of substrates (Si, Be, and glass) in a plasma chamber operated in the reactive-ion etching (RIE) mode using 1,3-butadiene gas at a pressure of 20 m Torr.[9] Films 50 and 200 nm thick were deposited at two self-bias voltages (-400 and -800 V). These two sets of samples were then ion beam implanted with 200-keV C^+ ions at doses ranging from 1×10^{14} to 1×10^{17} ions/cm^2, leaving part of the film areas unimplanted for comparison. The implant energy was chosen to send the ions through the film and into the substrate. Film samples were also thermally annealed using the RTA technique at temperatures up to 800 °C for 20 s in argon.

Several analytical methods were used to characterize the modified films. Hydrogen content was determined using elastic recoil detection (ERD) analysis[10] with a 1.66-MeV He^+ beam incident at a grazing angle (15°) to the sample. Rutherford backscattering was used to determine the carbon content of the films as a function of implanted ion dose. The ERD and RBS data were combined to obtain a [C]/[H] ratio. Raman spectra were obtained with a microprobe apparatus described in detail elsewhere.[11] The exciting radiation was provided by an Ar^+ laser tuned to the 5145-Å line. All spectra were taken in the backscattering configuration; the scattered light was not analyzed for polarization because of the amorphous nature of the films. Data taken at various spots ≈ 1 μm in diameter gave the same results, indicating uniformity on this scale. Optical-absorption and electrical resistivity measurements were also made.

III. RESULTS

The hydrogen content versus ion-beam dose is shown in Fig. 1 for films obtained at a bias of -400 and -800 V. Although the initial hydrogen content in the film obtained at a lower bias is higher (atomic ratio [C]/[H]=2.9 versus 4.6 for the -800-V film), the hydrogen concentration in both films implanted with the maximum dose (1×10^{17} ions/cm^2) is nearly the same (atomic ratio [C]/[H]=12.2 versus 13.4). Similar H concentrations

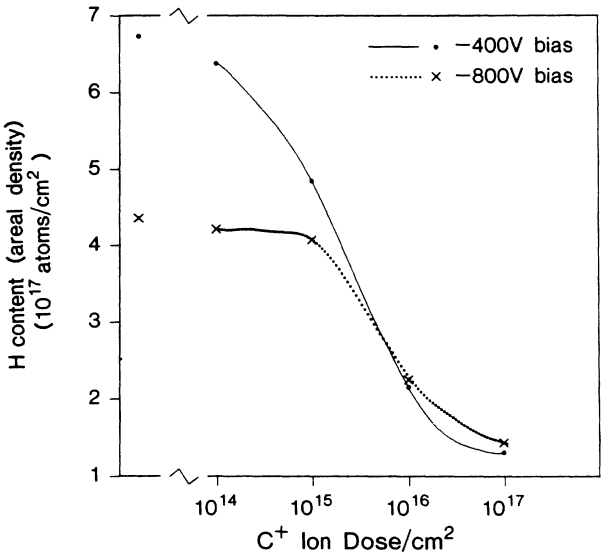

FIG. 1. Hydrogen content vs ion-beam dose for films deposited from 20 m Torr of 1,3-butadiene at −400 and −800 V. Solid and dotted curves are spline fits to guide the eye.

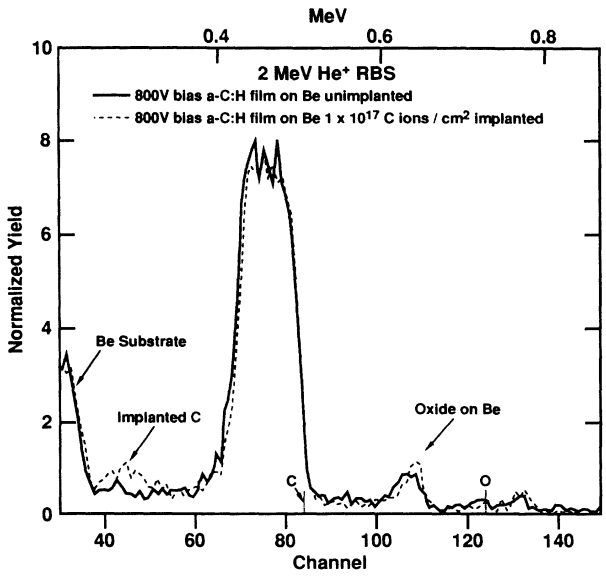

FIG. 2. Typical RBS spectrum showing C peak before and after maximum implant dose (10^{17} cm^{-2}).

([C]/[H]=12) were achieved for films RTA processed at a temperature of 800 °C. No measurable H loss occurred at temperatures below 300 °C.

A polystyrene film of known thickness was used as a standard in the ERD experiment. Since the ERD measurements yield the hydrogen area density in atoms/cm^2, a knowledge of the film density, its thickness and carbon content is required to obtain the ratio [C]/[H]. The film thickness measured with an Alpha Step 200 profilometer was 199±3 nm for the sample obtained at the −400-V bias and 207±3 nm for the film grown at −800-V bias. Film thickness decreased by ≈10% at the highest implant dose. This reduction was comparable to that indicated by the RBS profile of carbon measured before and after implantation at a dose of 1×10^{17} ions/cm^2. Figure 2 shows a typical RBS spectrum where a fit of the carbon peak is made using the results of the ERD measurements and the RUMP backscattering simulation program.[12] Table I gives the film compositions ([C]/[H] ratios) as well as film densities which have been calculated from the profilometer thickness and areal density measurements (ERD and RBS). The density measurements could be affected by the presence of voids, but previous TEM studies have shown their absence in similar systems.[13]

Although a significant reduction of hydrogen content resulted from the implantation process, the films retained their adhesion to the substrate (borosilicate glass substrates were an exception as they caused poor adhesion both before and after implantation) and their hardness was about 8 on the Mohs scale. However, it was clearly visible that even at the intermediate doses the reflectivity of the films was rapidly increasing until they appeared

TABLE I. Characteristics of *a*-C:H films as a function of C^+ ion dose. Asterisks denote numbers calculated using extrapolated values of RBS and ERD thickness between the points measured at 0 dose and maximum implant dose (10^{17} cm^{-2}).

Bias (V)	Dose cm^{-2}	[C]/[H] ratio	Thickness RBS and ERD (10^{18} atoms/cm^2)	Thickness alpha step (Å)	Density (10^{22} atoms/cm^3)
−400	0	2.9	1.95	1993±30	9.8
	10^{14}	2.9*			
	10^{15}	3.6*			
	10^{16}	7.8*			
	10^{17}	12.2	1.60	1768±30	9.0
−800	0	4.6	2.00	2070±30	9.7
	10^{14}	4.6*			
	10^{15}	4.6*			
	10^{16}	7.9*			
	10^{17}	13.4	1.70	1840±30	9.2

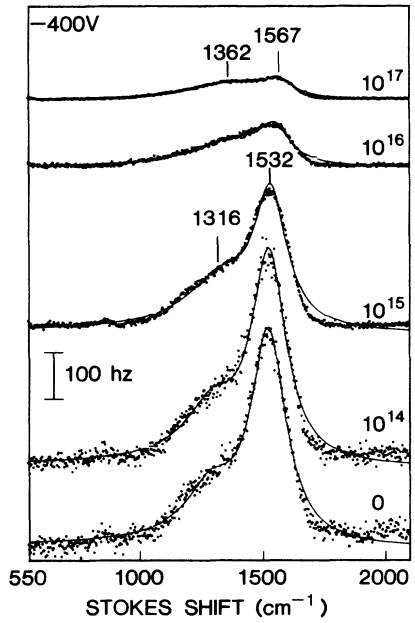

FIG. 3. Raman spectra of plasma deposited carbon films grown at −400-V self-bias. The number to the lower right of each spectrum indicates C^+ ion dose/cm^2; the unirradiated film is labeled 0. The points indicate the raw data and the solid lines are the fitted curves according to Eq. (1) in the text.

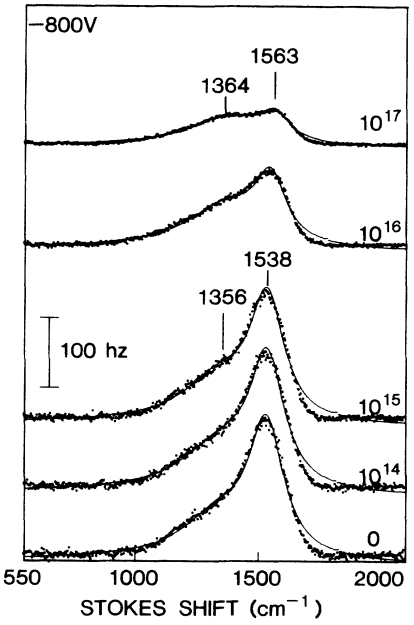

FIG. 4. Same as Fig. 3 for films grown at a self-bias of −800 V.

metallic at the maximum dose.

Raman spectra of the films deposited at two different self-bias voltages are presented in Figs. 3 and 4 as a function of the C^+ implant dose. In each figure, the data points are presented along with a computer fit which takes into account the possible asymmetry of the line shapes. The form used is given by Dillon *et al.*[5] as

$$\frac{dI}{d\omega}=K\frac{\Gamma\omega_0}{(\omega_0^2-\omega^2)^2+4\Gamma^2\omega_0^2\omega^2}\ , \tag{1}$$

where $dI/d\omega$ gives the Raman scattering intensity at frequency shift ω, ω_0 is the undamped mode frequency, Γ is a damping constant, and K is a constant of proportionality. The sum of two such lines was used to fit the data for the unirradiated films and those exposed to ion doses ranging from 10^{14} to 10^{17} ions/cm^2. K, Γ, and ω_0 for each line were used as fitting parameters; the program was based on a variable-projection technique combined with a variation of Newton's method.[14,15]

Single-crystal graphite exhibits a Raman spectrum consisting of a single line[16] at 1580 cm^{-1}. Theoretical calculations[6] reproduce this spectrum for an assembly of carbon atoms having only trigonal bonds at the ideal bond angle of 120°. When small microcrystallites form, or when bond-angle disorder is introduced, the graphite, or G line, shifts down to lower frequencies and broadens;[5,6] another line, the D or disorder line, begins to grow at a value calculated[6] to be 1310 cm^{-1}. The data and analysis

TABLE II. Parameters of Eq. (1) obtained by fitting G and D lines simultaneously to the Raman spectra of Figs. 3 and 4.

		G			D		
Bias (V)	Dose (cm^{-2})	ω_0 (cm^{-1})	Γ	Δ (FWHM) (cm^{-1})	ω_0 (cm^{-1})	Γ	Δ (FWHM) (cm^{-1})
−400	0	1528±1	0.0568±0.0011	175±4	1298±8	0.0930±0.0043	244±13
	10^{14}	1530±1	0.0558±0.0010	171±3	1305±7	0.0976±0.0042	257±13
	10^{15}	1537±1	0.0522±0.0010	161±4	1345±7	0.119±0.003	324±11
	10^{16}	1552±2	0.0495±0.0019	154±7	1394±6	0.132±0.003	374±9
	10^{17}	1570±2	0.0465±0.0014	147±5	1385±4	0.127±0.002	358±8
−800	0	1537±2	0.0560±0.0012	173±4	1357±10	0.125±0.003	345±12
	10^{14}	1539±2	0.0564±0.0013	174±4	1358±10	0.128±0.003	353±12
	10^{15}	1539±2	0.0551±0.0011	170±4	1352±8	0.122±0.004	330±12
	10^{16}	1551±2	0.0501±0.0014	156±5	1385±6	0.130±0.003	368±8
	10^{17}	1566±2	0.0462±0.0015	145±5	1387±4	0.126±0.002	356±9

presented in Figs. 3 and 4 and Table II show that both lines are present in unexposed, as-deposited films. The *G* line position is approximately the same in Figs. 3 and 4, but the *D* line is at a lower wave number position for the −400-V bias case. This may be due to the fact that the films initially deposited at a lower bias contain a larger amount of hydrogen and a larger proportion of tetragonal bonds. It should be noted that theoretical calculations for purely trigonal bonds lead to a value of 1310 cm^{-1} for the *D* line, which does not appear to be a function of bond disorder.[6]

As can be seen from Table II, the positions and widths of the *G* and *D* lines as found for the films made at −400-V bias are the same for the unirradiated film and the film receiving the 10^{14}-cm^{-2} dose. This correlates well with the constancy of the [C]/[H] ratio (Table I). As this ratio increases, the *G* and *D* line positions shift to higher frequencies, the *G* linewidth narrows, and the *D* linewidth increases. This correlation with [C]/[H] ratio also holds for the films made at −800-V bias: the *G* and *D* linewidths and positions remain constant up to doses of 10^{15} cm^{-2} as does the [C]/[H] ratio. The *D* line positions are greater for the doses just specified for the −800-V films than for the −400-V films and the *D* linewidths are greater for the −800-V films, correlating with the greater [C]/[H] ratio for the −800-V films. The [C]/[H] ratio is the same for both −400- and −800-V films at doses of 10^{16} and 10^{17} cm^{-2}; as a result, linewidth and position for both *G* and *D* lines are the same for both biases at these doses. Thus the greater the amount of hydrogen, the higher the proportion of tetragonal bonds and the narrower the width of the *D* line. As hydrogen is released with higher ion dose, the *G* linewidth narrows because of the transition to trigonal bonding, in agreement with theory.[6] Previous work[5] shows a similar upward shift of ω_0 and decrease in *G* linewidth as carbon films are annealed at increasing temperatures.

The calculated density of states of pristine graphite[17] has peaks at 1624 and 1345 cm^{-1}. These peaks are shifted and broadened for various models of amorphous carbon.[6] The Raman spectrum of *a*-C:H films exposed to increasing doses of 200 keV C^+ increasingly resembles the phonon density of states rather than being restricted to modes at the center of the Brillouin zone as wave-vector conservation is destroyed. This condition occurs as a function both of bond disorder and crystallite formation. Thus we associate the *G* peak at $\approx$1530–1600 cm^{-1} (see Tables II and III) with the calculated graphite density of states peak at 1624 cm^{-1}, and the *D* line at $\approx$1300–1400 cm^{-1} with the 1345-cm^{-1} peak. We have seen no evidence for the 700-cm^{-1} band reported by Parmigiani *et al.*[18]

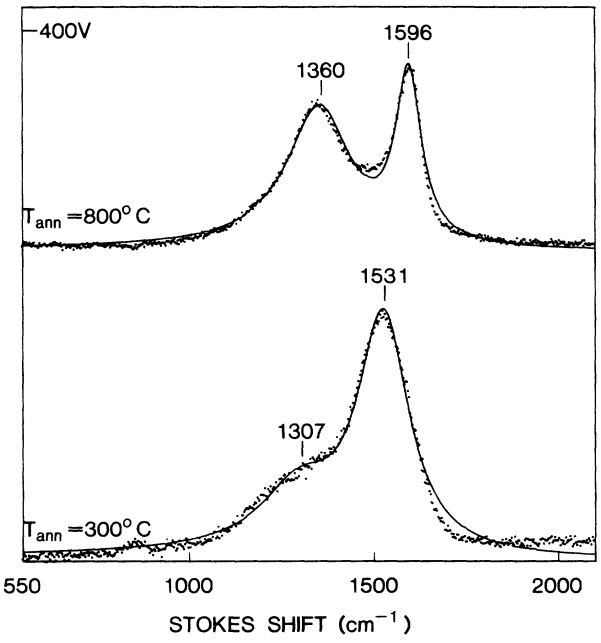

FIG. 5. Raman spectra of films grown at −400-V self-bias and annealed at 300 and 800 °C. Points and solid lines as in Fig. 3.

Figures 5 and 6 show the Raman spectra of these films for each deposition self-bias voltage after annealing at 300 and 800 °C. The data were fit as before, and Table III summarizes the results. The positions and widths of the *G* and *D* peaks agree well with previous work.[5]

Figure 7 shows the ratio of the intensity of the *D* and *G* bands, obtained by numerical integration of the band shapes of Figs. 4 and 5 as given by Eq. (3). Consistent with previous results, very little change occurs until a dose of 10^{16} cm^{-2} is reached, when $I(D)/I(G)$ shows a rapid increase. A similar effect has been reported in annealed carbon films where it was attributed to a growth in size and number of crystallites.[5]

Four-probe electrical resistivity measurements were carried out only for samples implanted with the two highest doses of 200 keV C^+ ions [the resistance was above our measuring range ($>10^{12}$ Ω cm) for doses of

TABLE III. Parameters of Eq. (1) obtained by fitting *G* and *D* lines simultaneously to the Raman spectra of Figs. 5 and 6.

Bias (V)	Anneal temperature °C	*G* ω_0 (cm^{-1})	*G* Γ	*G* Δ (FWHM) (cm^{-1})	*D* ω_0 (cm^{-1})	*D* Γ	*D* Δ (FWHM) (cm^{-1})
−400	300	1531±1	0.0556±0.0008	170±3	1307±6	0.0939±0.0031	245±9
	800	1596±1	0.0261±0.0004	83±1	1360±1	0.0772±0.0010	210±3
−800	300	1539±1	0.0555±0.0010	171±3	1352±8	0.123±0.004	332±12
	800	1588±2	0.0284±0.0006	90±2	1370±2	0.110±0.002	300±5

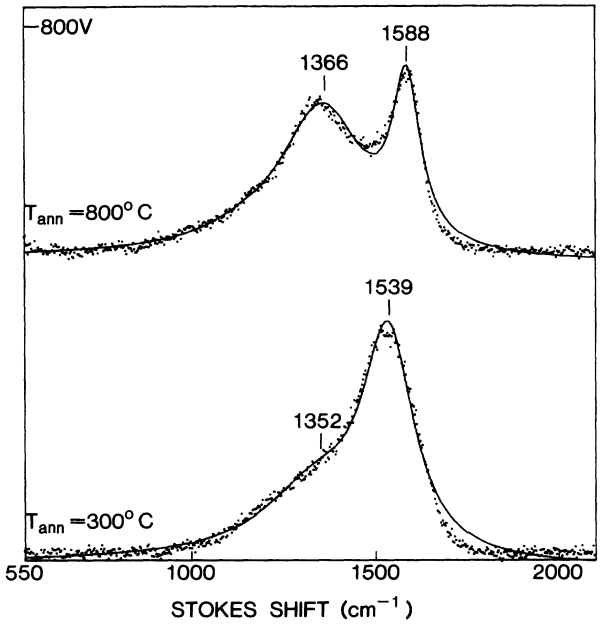

FIG. 6. Same as Fig. 6 for films grown with self-bias of −800 V.

1×10^{15} and lower]. The resistivity decreases by 3 orders of magnitude from >100 Ω cm to <0.1 Ω cm in the range measured and is rapidly approaching the value for graphite ($\approx1\times10^{-3}$ Ω cm). Figure 8 shows optical-absorption spectra for the −400-V bias samples in the range of 300 to 2000 nm. These data show, as was the

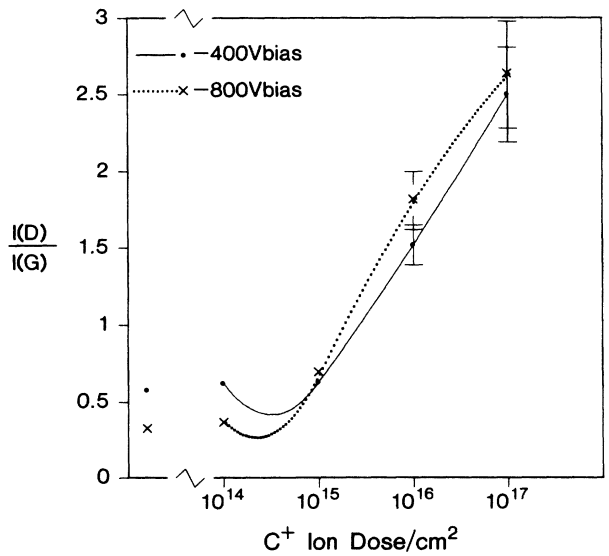

FIG. 7. Ratio of the integrated intensities of the *D* and *G* lines as a function of ion dose corresponding to Raman spectra of Figs. 3 and 4. Where error bars are not specifically shown, they are no larger than the magnitude of the symbol. The solid and dotted curves serve only as a guide to the eye.

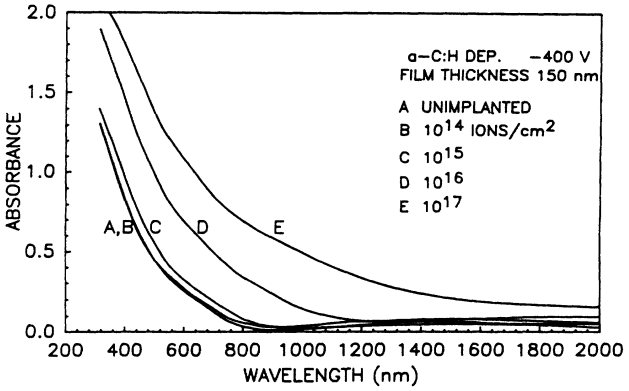

FIG. 8. The effect of implantation with 200-keV C$^+$ ions on the optical density of *a*-C:H films formed with −400-V bias as a function of ion dose.

case in the above-described experiments (i.e., ERD, Raman, etc.), *that the major changes occur in the a-C:H films implanted with doses* $>10^{16}$ *cm*$^{-2}$, thus indicating a correlation between the reduction of hydrogen content and the optical and electronic properties.

IV. DISCUSSION

The properties of the as-deposited films depend mostly on the impact energy of the hydrocarbon fragments which is determined by the gas pressure and rf bias voltage.[9] Thus the lower initial hydrogen content in the −800-V sample is a consequence of the more efficient bond breaking and hydrogen removal at the higher energy of incoming ion flux than in the −400-V case. IR studies have shown that the ratio of tetragonal to trigonally bound carbon in similar films plasma deposited from benzene was about 2:1.[19] Other studies have suggested that a significant proportion of hydrogen may be unattached to the carbon and may possibly be bound in clusters[20] or perhaps intercalated into turbostratic graphite layers.[21] The simplest model, which has the highest consistency with published data, describes the *a*-C:H structure as a random network of covalently bonded carbon in some proportion of tetragonal to trigonal coordination with some bonds being terminated by hydrogen atoms.[6,19,22] Thus films of the type discussed here are similar to amorphous carbon and are not polymeric in nature.

The 200-keV C$^+$ ions create secondary electrons along their damage tracks, which are ≈1 nm in diameter; these electrons break the covalent bonds in the film and create free H, C, and possibly small amounts of various CH fragments.[23] At the high energy of the implanted species there are few nuclear collisions in the film and the implanted ions come to rest well into the substrate. The electronic energy imparted to the film is in the range of 50 eV Å. The continued accumulation of flux gives a cumulative damage effect, but the actual damage tracks never overlap as the lifetime of the individual collision is $\approx10^{-11}$ s,[24] much shorter than the dose rate during the implantation. The resulting free hydrogen atoms diffuse

out of the film and carbon atoms remain behind, recombining to the lowest stable binding configuration which is trigonal.

The decrease in hydrogen content with dosage found here is in agreement with results recently reported using other species of ions in the bombardment.[7,8] It was also found that resistance is lowered as the films are increasingly graphitized.[7] The extensive photoluminescence data reported by Gonzalez-Hernandez *et al.*[8] have superimposed on it the Raman peak near the expected graphite position, but this feature was not examined in any detail.

The ion-implantation results presented here are comparable to those achieved using thermal annealing,[5] where it is well established that bonded hydrogen is released between 400 and 600 °C (Ref. 12) and that a tetragonal to trigonal bonding transition occurs for the carbon network. It should be noted, however, that our film samples were deposited in the absence of heating (less than 100 °C during implantation) indicating that although the mechanisms are different, thermal annealing and ion-beam implantation produce similar compositional and structural changes in *a*-C:H films. However, the width of the *G* peak for the heat-treated films is less than that of the *G* peak measured on the ion-implanted samples, which implies that the heat treatment leads to the growth of larger crystals than are found in the ion-bombarded films.

It is also interesting to compare these results to similar work done in ion-beam irradiated polymer films.[23] These films were found to lose a significant fraction of their original carbon content (40%) and reached somewhat lower resistivities (1×10^{-3} Ω cm at a dose of 1×10^{17} ions/cm^2) indicating a faster rate of graphitization. The above results can be explained by the structural differences between polymer materials composed of weakly bound linear chains with a high H:C ratio resulting in partial volatilization of the hydrocarbon fragments and compounds, and the highly crosslinked, low-hydrogen-content *a*-C:H films.

The final point to note is the small difference between the densities of the films before and after implantation at a dose of 1×10^{17} ions/cm^2 as shown in Table I. Generally, it is accepted that the incorporation of hydrogen into *a*-C:H films lowers their density by reducing the degree of crosslinking of the carbon matrix. The above data show here the opposite effect, i.e., a decrease in density with a decrease in hydrogen content. It appears that there are two competing processes responsible for the observed density changes. Aside from the possibility of void formation mentioned previously, a potential increase in density due to a lower hydrogen content could be offset by the transition from tetragonal to the less dense threefold bonding configuration of the carbon atoms.

V. CONCLUSIONS

Implantation of amorphous hydrogenated carbon films with 200-keV C^+ ions resulted in a dose-dependent significant reduction of hydrogen content in the films as measured by RBS and ERD techniques. Optical absorption, Raman spectroscopy, and electrical resistivity give evidence of increasing graphitization as a function of dose, with major changes occurring for doses of 10^{16} cm^{-2} and greater. These results parallel those found for thermally annealed *a*-C:H films for which hydrogen loss has been observed to occur above ≈400 °C.

[1] S. Kasi, H. Kang, and J. W. Rabalais, Phys. Rev. Lett. **59**, 75 (1987).

[2] K. E. Spear, *Earth and Mineral Sciences* (Pennsylvania State University, University Park, PA, 1987), Vol. 56, p. 53.

[3] H. Tsai and D. B. Bogy, J. Vac. Sci. Technol. A **5**, 3287 (1987).

[4] J. C. Angus, P. Koidl, and S. Domitz, in *Plasma Deposited Thin Films*, edited by J. Mort and F. Jansen (CRC, Florida, 1986), p. 89.

[5] R. O. Dillon, J. A. Woollam, and V. Katkanant, Phys. Rev. B **29**, 3482 (1984).

[6] D. Beeman, J. Silverman, R. Lynds, and M. R. Anderson, Phys. Rev. B **30**, 870 (1984).

[7] D. C. Ingram and A. W. McCormick, Phys. Res. B **34**, 68 (1988).

[8] J. Gonzalez-Hernandez, R. Asomoza, A. Reyes-Mena, J. C. Rickards, S. S. Chao, and D. Pawlik, J. Vac. Sci. Technol. A **6**, 1798 (1988).

[9] A. S. Gozdz, P. S. D. Lin, A. Scherer, and S. S. Lee, Electron. Lett. **24**, 123 (1988).

[10] J. L'Ecuyer, C. Brassard, C. Cardinal, J. Chabbal, L. Deschênes, and J. P. Labrie, J. Appl. Phys. **47**, 381 (1976).

[11] J. B. Hopkins and L. A. Farrow, J. Appl. Phys. **59**, 1103 (1986).

[12] L. Doolittle, Nucl. Instrum. Methods P **9**, 344 (1985).

[13] D. C. Ingram, J. A. Woollam, and G. Bu-Abbud, Thin Solid Films **137**, 225 (1986).

[14] J. E. Dennis, D. M. Gay, and R. E. Welsch, ACM Trans. Math. Software **7**, 348 (1981).

[15] L. Kaufman, BIT **15**, 49 (1975).

[16] R. Tuinstra and J. L. Koenig, J. Chem. Phys. **53**, 1126 (1970).

[17] R. Al-Jishi and G. Dresselhaus, Phys. Rev. B **26**, 4514 (1982).

[18] F. Parmigiani, E. Kay, and H. Seki, J. Appl. Phys. **64**, 3031 (1988).

[19] B. Dischler, A. Bubenzer, and P. Koidl, Solid State Commun. **48**, 105 (1983).

[20] J. R. Reimger, R. W. Vaughan, J. R. Knights, and R. A. Lujan, J. Vac. Sci. Technol. **19**, 53 (1981).

[21] R. H. Bragg, Synth. Met. **7**, 95 (1983).

[22] S. Craig and G. L. Harding, Thin Solid Films **97**, 345 (1982).

[23] T. Venkatesan, S. R. Forrest, M. L. Kaplan, C. A. Murray, P. H. Schmidt, and B. J. Wilkens, J. Appl. Phys. **54**, 3150 (1983).

[24] L. M. Howe, M. H. Rainvill, H. K. Harigan, and D. A. Thompson, Nucl. Instrum. Methods **54**, 3150 (1983).